MATHEMATICAL ANALYSIS OF OPEN SPACE INTERFERENCE CANCELLATION MODEL IN EMC MEASUREMENT

Fahim Gohar Awan, Noor Muhammad Sheikh, Asima Kiran
Faculty of Electrical Engineering, UET, Lahore, Pakistan
Contact: fahimgohar@hotmail.com

ABSTRACT *— In this paper a deterministic model for cancelation of interference in an open space is presented along with its architecture, and various attributes of the environment. The basics of the adaptive algorithmic technique in a classic practical scenario are analyzed. A notable feature of the model is that it allows for the importation of the serious challenge for measurement at open site posed by random interfering sources. The presence of licensed RF operators almost anywhere within the whole spectrum of interest or a broadband interferer e.g., digital broadcast transmitter may pollute EM emission measurements. An analytical solution to the stringent conditions put up by these issues in the design of interference cancelation model at open space is described. Rigorous analysis validates the model for the range of frequency and shows that it is asymptotically stable.*

Index Terms — Electromagnetic compatibility (EMC), Interference cancellation, Open area test site (OATS).

I. INTRODUCTION

The field of electromagnetic compatibility deals with the analysis and mitigation of the undesired radiated EM fields and/or conduction voltages/currents. These unwanted signals interact with other electronic devices and systems within their range. System performance of these electronic devices may get badly affected by absorbing the conducted or radiated energy generated by various sources, present within their ambient environment range. One such example is EM interference where a system malfunctions or start radiating EM energy.

There are two ways of energy coupling between two electronic devices (source and receiver) viz radiated coupling and conducted coupling. In radiated coupling radio wave energy is propagated either through gaseous medium or air. Whereas energy signal is fed through interconnecting link wires in conducted coupling. Figure 1 shows a conventional electromagnetic radiated emission setup for measuring desired equipment under test (EUT) emissions at OATS. Where d is the intentional source-receiver distance and N is the number of unwanted ambient interfering sources. The received signal comprise of blue arrow i.e., intentional EUT signal plus crossed arrows i.e., contribution from N un-intentional ambient interferers each with unique distance, angle and position.

To date equipment uses either stepped frequency of sweep frequency for frequency domain radiated emission measurement of electronic system. But this technique is helpful for the investigation of narrow band signals that are continuous in time. Whereas impulsive signals are difficult to measure precisely. This shortcoming has been overcome using conventional peak-hold detector and by taking multiple sweeps of high frequency signal measuring peaks of the spectrum. The disadvantage of this technique is its longer recording and measurement time. Further it does not record all possible peak emissions due to pause during system capturing time.

EM interference (EMI) measurement in open space has attracted researcher in the recent years. A frequency domain ambient interference cancellation has been introduced in [1] by using time-dividing technique (EUT On-Off). The drawback of such a system is the consistency of the interfering signals present in the vicinity during the capturing time intervals. [2] suggested recording of frequency domain snap shots at two different yet pre-determined test locations and then applying superposition theory for cancellation of unwanted interference signal.

During classical era, adaptive noise cancellation techniques were evolved. Making use of this algorithm in EMC, some ambient interference cancellation methods are suggested in literature [4], [5]. These methods were based on conventional EMC measuring equipment and largely have the common drawback of extended record and capture time [6].

In this paper a novel deterministic model for radiated emission measurement is proposed and analyzed. The receivers are conditioned for higher directivity during data acquisition that in essence guarantees the complete isolation of two intended signal streams (EUT signal and composite signal). The interference cancellation model is successfully simulated in MATLAB environment in time domain [7]. The algorithm is applied on data blocks acquired in real time, thus significantly lowering the processing time.

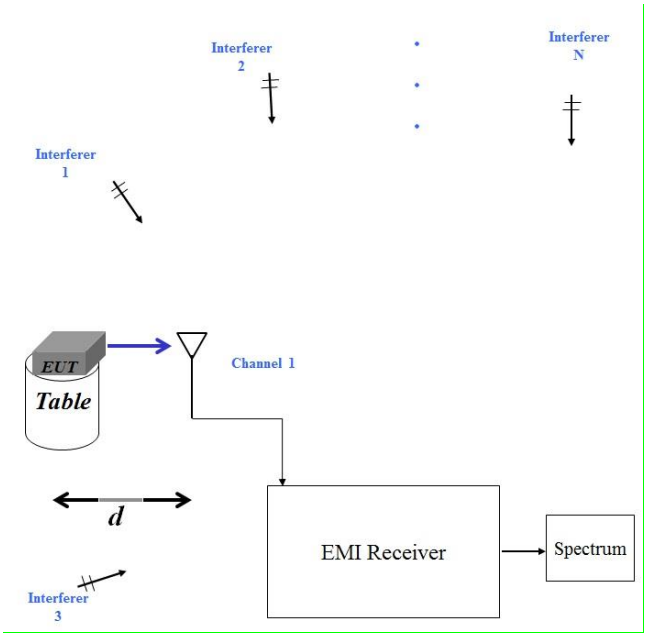

Figure 1. Conventional EMI measurement set up

The next section describes the analytical model exposed to various stringent conditions in open space over a range of frequencies of interest (FOI) for its validation.

II. MODEL FORMULATION

Assumptions

Following are the key assumptions for proper functioning of the proposed technique at open area test site.

- The resultant interferences at both of the antenna ports are in high degree of correlation whereas EMI emissions radiated by EUT are uncorrelated with this resultant interference.
- EUT power spectrum is assumed to be stationary, at least in the wide sense, during the sample acquisition time.
- EUT signal is wide-sense stationary (WSS) during the calculation time of FFT for estimation of a signal's spectral characteristics.
- EUT emissions fall in the main lobe of Antenna 2 whereas antenna 1 is in the back lobe of antenna 2. There is complete isolation between the main lobs of the two antennas.
- Sources of Interference are far away from both antennas with little ground reflections and the environment is free from reflecting objects such that the interfering signals can be assumed as plane wave.
- The noise is considered to be additive white Gaussian noise (AWGN) with mean zero. Further the noise power is much below that of EMC measurements and the power level of interference signal.

Methodology

Two receiving antennas are adopted marking channel 1 as primary antenna and channel 2 as reference antenna. Both antennas have to be synchronous (with identical pattern) and displaced by distance D. EUT is placed at a distance d from reference channel as shown in figure 2. The two antennas are displaced beyond $2 \times d$ for lowering the signal power entering the second channel. Signal at both channels are captured and recoded at the same time and the proposed interference cancellation algorithm is employed in real-time.

Since the two receiving antennas are placed at different locations, the received signals will exhibit time and phase mismatch on the two ports of antennas. This may become serious in case any interfering signal does not reach the second antenna and may therefore be wrongly interpreted as emissions from EUT. Therefore it calls for some kind of remedy for two streams to be in synchronization. As the setup is defined for open space under the influence of unknown radiators, it has to be configured each time for a new set of observations irrespective of whether the distance D is kept the same.

In order to analyze the effect of same signal received at two ports of antenna with different phase, consider the angle of arrival θ and phase angle φ of the arriving interference wave to be random variables as shown in Figure 3. Angle of arrival θ is limited to ± 20 degrees in correspondence with the half power beamwidth of the two selected antennas. For

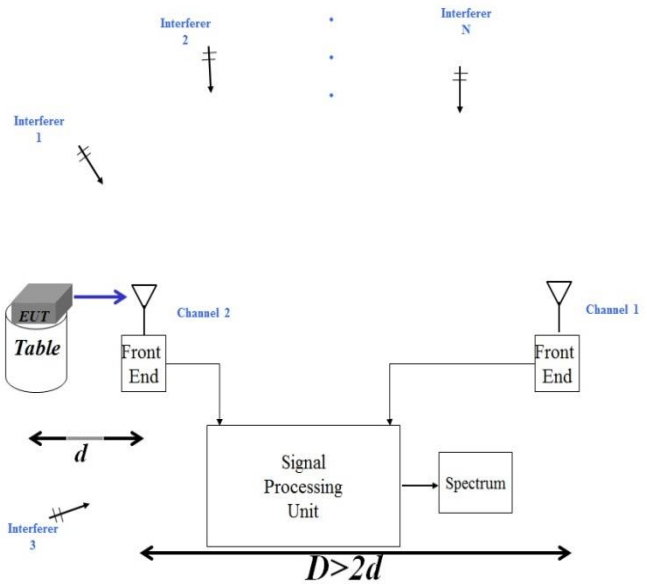

Figure 2. A schematic of Over the Air Interference approximation model

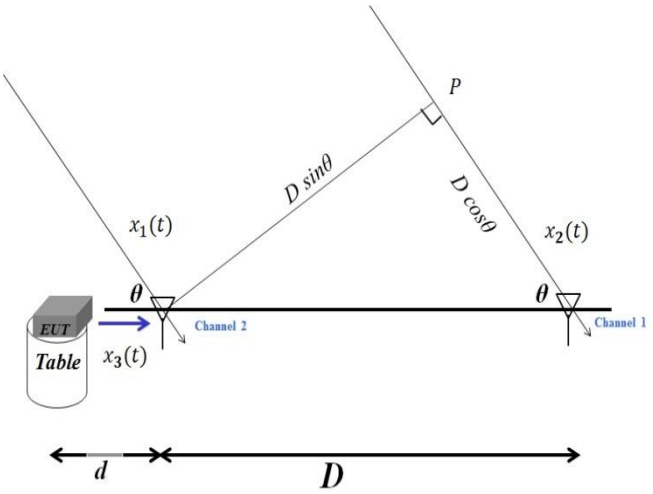

Figure 3: Difference in path length and phase for two ray model

angles beyond this, the interfering signal contribution on the antennas is assumed to be negligible. For the frequency of interest (0.1 – 1) GHz, the corresponding wavelength λ will be (0.3-3.0) m.

Case I: *EUT off. i.e., without EUT emissions*

Let us assume a plane wave having an arbitrary frequency ω arriving from certain elevation imposes two signals $x_1(t)$ on channel 2 and $x_2(t)$ on channel 1 as shown in Figure 3.

$$x_1(t) = Ae^{j(\omega t+\varphi)}, \quad (1)$$

$$x_2(t) = Be^{j(\omega t+\varphi+\frac{2\pi}{\lambda}.Dcos\theta)}, \quad (2)$$

Adding the two signals of the two channels results in

$$x(t) = x_1(t) + x_2(t)$$
$$= Ae^{j(\omega t+\varphi)} + Be^{j(\omega t+\varphi+\frac{2\pi}{\lambda}.Dcos\theta)}, \quad (3)$$

For calculating power of this resultant signal, the expected value will be

$$p(t) = E[x(t).x^*(t)]$$
$$= E[[x_1(t) + x_2(t)].[x_1(t) + x_2(t)]^*], \quad (4)$$
$$= E\left[Ae^{j(\omega t+\varphi)} + Be^{j\left(\omega t+\varphi+\frac{2\pi}{\lambda}.Dcos\theta\right)}\right].\left[Ae^{-j(\omega t+\varphi)} + Be^{-j\left(\omega t+\varphi+\frac{2\pi}{\lambda}.Dcos\theta\right)}\right], \quad (5)$$
$$= E\left[A^2 + B^2 + ABe^{-j\frac{2\pi}{\lambda}.Dcos\theta} + ABe^{j\frac{2\pi}{\lambda}.Dcos\theta}\right], \quad (6)$$
$$= E\left[A^2 + B^2 + 2AB.\cos(\frac{2\pi}{\lambda}.Dcos\theta)\right] = E[g(\theta)], \quad (7)$$

(where $x^*(t)$ is the complex conjugate of $x(t)$). Assuming uniform angular distribution of interference signal, the average power of the resultant signal will be

$$= \frac{9}{2\pi}.\int_{-\pi/9}^{\pi/9} g(\theta).d\theta, \quad (8)$$

Therefore, the average power will become

$$= \frac{1}{2\pi/9}.\int_{-\pi/9}^{\pi/9}.\left[A^2 + B^2 + 2AB.\cos(\frac{2\pi}{\lambda}.Dcos\theta)\right].d\theta, \quad (9)$$

After simplification,

$$= A^2 + B^2 - \frac{2.66AB\lambda}{D}\sin\frac{5.9D}{\lambda}, \quad (10)$$
$$= A^2 + B^2 - \frac{2.66AB\lambda}{D}\sin\frac{5.9fD}{c}, \quad (11)$$

where c is speed of light. If we assume no loss of wave amplitude at the two receivers, i.e., $A = B$ then

$$= A^2[2 - \frac{2.66\lambda}{D}\sin(5.9\frac{fD}{c})], \quad (12)$$

This means that the power of the incoming interfering signal depends only on the separation D between the two antennas and its frequency of operation but not on its phase.

Case II: *EUT perpendicular to two receiving antennas*

As per EMC requirements, ground reflections must be included in its measurements and for the second antenna which records the interference signal only, these ground reflections must be avoided. Therefore the orientation of the EUT and antennas are changed and placed perpendicular to an earlier position i.e., EUT signal is in the main lobe of antenna 2 whereas EUT signal is not pouring into the major lobe of antenna 1 as shown in Figure 4. In this case The phase difference of the two signals is

$$\varphi_1 - \varphi_2 = \frac{2\pi}{\lambda}Dsin\theta, \quad (13)$$

To see the effect of random interfering sources on the EUT emissions, the difference of these signals from the two antenna ports at channel 2 will be

$$x(t) = x_1(t) - x_2(t)$$
$$= Ae^{j\left(\omega t+\varphi+\frac{2\pi}{\lambda}.Dsin\theta\right)} - Ae^{j(\omega t+\varphi)}, \quad (14)$$

For calculating power of the difference signal $x(t)$, the expected value will be

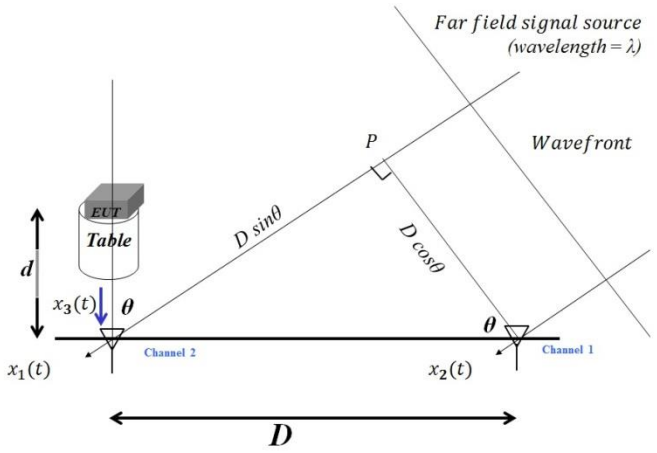

Figure 4: EUT placed perpendicular to receiving antennas. EUT emissions and EUT ground reflection are captured in channel 2 only.

$$p(t) = E[x(t).x^*(t)]$$
$$= E[[x_1(t) - x_2(t)].[x_1(t) - x_2(t)]^*], \quad (15)$$
$$= E\left[Ae^{j\left(\omega t+\varphi+\frac{2\pi}{\lambda}.Dsin\theta\right)} - Ae^{j(\omega t+\varphi)}\right].\left[Ae^{-j\left(\omega t+\varphi+\frac{2\pi}{\lambda}.Dsin\theta\right)} - Ae^{-j(\omega t+\varphi)}\right], \quad (16)$$
$$= E\left[A^2 + A^2 - A^2e^{-j\frac{2\pi}{\lambda}.Dsin\theta} - A^2e^{j\frac{2\pi}{\lambda}.Dsin\theta}\right], \quad (17)$$
$$= E\left[2A^2 - 2A^2.\cos(\frac{2\pi}{\lambda}.Dsin\theta)\right] = E[g(\theta)], \quad (18)$$

Assuming uniform angular distribution, the average power of the resultant signal will be

$$= \frac{9}{2\pi}.\int_{-\pi/9}^{\pi/9} g(\theta).d\theta, \quad (19)$$

Therefore, the average power will become

$$= \frac{9}{2\pi}.\int_{-\pi/9}^{\pi/9}.\left[2A^2 - 2A^2\cos(\frac{2\pi}{\lambda}.Dsin\theta)\right].d\theta, \quad (20)$$

After simplification,

$$= 2A^2 - \frac{0.97A^2\lambda}{D}\sin\frac{2.15D}{\lambda}, \quad (21)$$
$$= A^2[2 - \frac{0.97\lambda}{D}\sin(\frac{2.15fD}{c})], \quad (22)$$

As shown in equation (13), to reach antenna at channel 2 the wave 1 has to travel extra distance $Dsin\theta$, resulting in the phase difference $\Delta\varphi$,

$$\lambda(\frac{\Delta\varphi}{2\pi} + I) = Dsin\theta, \quad (23)$$

Therefore, sin (Angle of arrival) is

$$\sin(AoA) = \frac{\lambda\left(\frac{\Delta\varphi}{2\pi} + I\right)}{D}, \quad (24)$$

where I is any positive integer value or zero and represents the number of full wavelengths the signal that goes along the extra length of path. When D is much smaller than the distance of the source of interference from antennas then the two incoming rays can be considered as parallel.

Case III: *Difference of power of signals*

Now consider the same two random WSS sinusoidal signals $x_1(t)$ and $x_2(t)$ and estimate the difference of their individual power.

$$P\big(x_1(t)\big) = E[x_1(t).x_1^*(t)], \tag{25}$$

$$= E\big[Ae^{j(\omega t+\varphi)}\big].\big[Ae^{-j(\omega t+\varphi)}\big] = A^2, \tag{26}$$

Similarly,

$$P\big(x_2(t)\big) = E[x_2(t).x_2^*(t)], \tag{27}$$

$$= E\left[Ae^{j\left(\omega t+\varphi+\frac{2\pi}{\lambda}.Dcos\theta\right)}\right].\left[Ae^{-j\left(\omega t+\varphi+\frac{2\pi}{\lambda}.Dcos\theta\right)}\right] = A^2, \tag{28}$$

This means that

$$P\big(x_1(t)\big) - P\big(x_2(t)\big) = 0, \tag{29}$$

Whereas

$$P\big(x_1(t) - x_2(t)\big) \neq 0, \tag{30}$$

Case IV: *With EUT emissions*

Now again consider a WSS time invariant signal $x_3(t)$ which is essentially EUT emissions and uncorrelated with both $x_1(t)$ and $x_2(t)$ signals.

From the observation in case III, it is observed that

$$P\big(x_3(t) + x_1(t) - x_2(t)\big) \neq P\big(x_3(t)\big) + P\big(x_1(t)\big) - P\big(x_2(t)\big), \tag{31}$$

Next we find the condition on these three signals under which power of the resultant signal on L.H.S i.e., obtained by subtracting $x_2(t)$ from composite signal $x_3(t) + x_1(t)$ at channel 2 is equal to the individual power of signal $x_3(t)$ on R.H.S.

Let

$$x_t(t) = x_3(t) + x_1(t) - x_2(t), \tag{32}$$

$$P\big(x_t(t)\big) = \overline{\big(x_3(t) + x_1(t) - x_2(t)\big)\big(x_3^*(t) + x_1^*(t) - x_2^*(t)\big)}, \tag{33}$$

$$\begin{aligned} P\big(x_t(t)\big) = {} & \overline{x_3(t)x_3^*(t)} + \overline{x_1(t)x_1^*(t)} + \overline{x_2(t)x_2^*(t)} \\ & + \overline{x_1(t)x_3^*(t)} + \overline{x_3(t)x_1^*(t)} - \overline{x_1(t)x_2^*(t)} \\ & - \overline{x_2(t)x_1^*(t)} - \overline{x_2(t)x_3^*(t)} \\ & - \overline{x_3(t)x_2^*(t)}, \end{aligned} \tag{34}$$

Since $x_1(t)$ and $x_3(t)$ are uncorrelated as well as $x_2(t)$ and $x_3(t)$ are uncorrelated. Therefore

In equation (34)

$$\overline{x_1(t)x_3^*(t)} = \overline{x_1(t)}\ \overline{x_3^*(t)}, \tag{35}$$

$$\overline{x_3(t)x_1^*(t)} = \overline{x_3(t)}\ \overline{x_1^*(t)}, \tag{36}$$

$$\overline{x_2(t)x_3^*(t)} = \overline{x_2(t)}\ \overline{x_3^*(t)}, \tag{37}$$

$$\overline{x_3(t)x_2^*(t)} = \overline{x_3(t)}\ \overline{x_2^*(t)}, \tag{38}$$

Now

$$\overline{x_1(t)x_3^*(t)} + \overline{x_3(t)x_1^*(t)} = 2\mathrm{Re}[\overline{x_1(t)x_3^*(t)}], \tag{39}$$

And

$$\overline{x_2(t)x_3^*(t)} + \overline{x_3(t)x_2^*(t)} = 2\mathrm{Re}[\overline{x_2(t)x_3^*(t)}], \tag{40}$$

From equations (39) and (40) and (34)

$$\begin{aligned} P\big(x_t(t)\big) = {} & P\big(x_1(t)\big) + P\big(x_2(t)\big) + P\big(x_3(t)\big) \\ & + 2\mathrm{Re}\big[\overline{x_1(t)x_3^*(t)}\big] - 2\mathrm{Re}\big[\overline{x_2(t)x_3^*(t)}\big] \\ & - \overline{x_1(t)x_2^*(t)} - \overline{x_2(t)x_1^*(t)}, \end{aligned} \tag{41}$$

If $x_1(t)$ can be made exactly equal to $x_2(t)$ by some means then equation (41) will yield $P\big(x_3(t)\big)$ as 4th and 5th terms $2\mathrm{Re}[\overline{x_1(t)x_3^*(t)}] - 2\mathrm{Re}[\overline{x_2(t)x_3^*(t)}]$ will be cancelled out and $P\big(x_1(t)\big) + P\big(x_2(t)\big) = \overline{x_1(t)x_2^*(t)} + \overline{x_2(t)x_1^*(t)}$.

Therefore,

$$P\big(x_t(t)\big) = P\big(x_3(t)\big), \tag{42}$$

This is only possible in case if phase delay of $\frac{2\pi}{\lambda}Dcos\theta$ is added to the signal that comes earlier at the antenna port. Thus phase compensation is mandatory to measure EUT emissions only in the presence of interference signals.

Maximum Ratio Combining:

Diversity combining techniques as used in wireless communication for improving signal to noise ratio can be employed here e.g., maximal ratio combining (MRC) technique since it synchronizes the phases of multiple copies of signal received at different antennas without a priori information of the spatial installation. The need for phase alignment in order to achieve diversity gain under joint interference scenario has been argued in [8], [9]. Multiple copies of same signal with two antennas setup have been aligned in [10] with the capability of real time processing with MRC. Authors in [11], [12] have proposed that MRC works significantly well for phase alignment under practical scenarios of imperfect channels in the presence of co-channel interference. Our problem of space diversity reception of same interfering source on two channels with unequal power and different phase angle is similar to their work; therefore MRC can be employed in our proposed design for measurement system for the sake of phase alignment of interfering sources only. Similarly authors in [13] investigated the performance of MRC in single input multiple output system with multi-element antennas and verified the correctness of the measurement taken in reverberation chamber. The time and phase alignment in MRC works as follows:

After sampling, the correlator differentiates between time domain and frequency domain received baseband signals as shown in Figure 5. The absolute magnitude values of the received baseband signals represented by complex scalar are computed that assist in calculating the difference between their peak positions. Following this the two streams $X_1(t)$ and $X_2(t)$ of signals are aligned in time domain by delaying or advancing, i.e. positioning $X_1(t)$ a time offset d with respect to $X_2(t)$. The phase difference between two streams of interfering signals $X_1(t) = R_1e^{j\theta_1}$and $X_2(t) = R_2e^{j\theta_2}$ is compensated by computing the phase offset $\varphi = angle\ (X_2{X_1}^*) = \theta_2 - \theta_1$, (where ${X_1}^*$ is the complex conjugate of X_1) and applying the negative to one of them or by bringing both of the individual phase to zero and applying a correction factors.

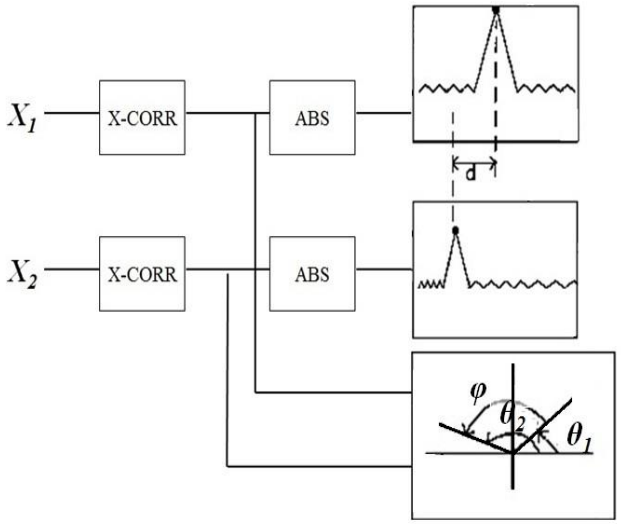

Figure 5: MIMO receiver with joint time-frequency domain MRC

Uniform Circular Array: For estimating Angle of Arrival

An improved version for evaluating the source of interference in measuring EUT emission would be obtained by using an array of antennas.

Consider an array of P antennas with identical characteristics placed uniformly with its phase centered in xy-plane to form a circular pattern of radius R. The antenna elements are uniformly polarized and pointing in the same direction. The azimuthal angle displacement of antennas is made according to $\varphi_t = (t-1)\frac{2\pi}{P}$ to obtain a circular symmetry as shown in Figure 6.

When Kplane waves hit the uniform circular array (UCA), the signal model of this array can be expressed as equation

$$\mathbf{x}(t) = \mathbf{A}(\theta,\varphi)\mathbf{s}(t) + \mathbf{n}(t), \quad (43)$$

where a set of space diversified vectors $\boldsymbol{a}(\theta,\varphi)$ from K element constitute $\boldsymbol{A}(\theta,\varphi)$ for $(k = 1 \ldots K)$. When a plane wave $\boldsymbol{E} = E\boldsymbol{u}_\theta + E\boldsymbol{u}_\varphi$ with direction of arrival $DOA(\theta,\varphi)$ strike the antenna array, the induced voltages are stored in the vector $\boldsymbol{a}(\theta,\varphi)$

$$\mathbf{a}(\theta,\varphi) = [a_1(\theta,\varphi), a_2(\theta,\varphi), \ldots, a_P(\theta,\varphi),]^T, \quad (44)$$

Since all the antennas have same polarization, the vector $\mathbf{a}$ depends only on its direction of arrival (θ,φ) and not on its polarization angle. The space diversified vector can be partitioned into its horizontal and vertical parts:

$$\mathbf{a}(\theta,\varphi) = \mathbf{a}_\theta(\theta,\varphi) + \mathbf{a}_\varphi(\theta,\varphi), \quad (45)$$

Where $\mathbf{a}_\theta(\theta,\varphi)$ and $\mathbf{a}_\varphi(\theta,\varphi)$ are the accumulated vertical and horizontal induced voltages contributions when a unit amplitude plane wave $\boldsymbol{E}$ strikes the array. The advantage of circular symmetry is that these induced voltages of distinctive antenna elements bear a relationship among them

$$a_t(\theta,\varphi) = a_1(\theta,\varphi-\varphi_t), \quad (46)$$

The mutual coupling outcome received on the antenna elements in a circular array varies their characteristics in comparison to the stand-alone characteristics mainly due to current induced from neighboring elements that changes the stand-alone radiation pattern of individual antenna element (shadowing and scattering effects). The model thus becomes complicated. However [14] showed that the induced voltage on impinging plane wave in the azimuth angle φ can be differentiated into limited phase modes over an antenna element in UCA.

$$a_1(\theta,\varphi) = \sum_{m=-M}^{M} a_m(\theta)e^{jm\varphi}, \quad (47)$$

The dimensions of the array restrict this expansion such that $M > \frac{2\pi d}{\lambda}$, where λ is the wavelength and d is the largest dimension of the circular array.

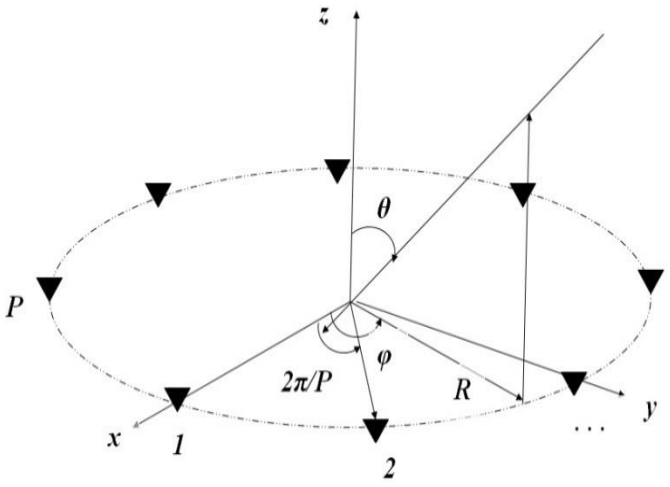

Figure 6: P antenna elements arranged symmetrically to form a uniform circular array

Now assume K plane waves strike the array at an elevation angle θ_0 which is fixed. Equation (47) thus describes the signal model of the uniform circular array where now

$$\boldsymbol{A}(\theta,\varphi) = [\mathbf{a}(\theta_0,\varphi_1), \mathbf{a}(\theta_0,\varphi_2), \ldots, \mathbf{a}(\theta_0,\varphi_K)], \quad (48)$$

The acquired data is then put through a beamspace transformation [15]

$$\mathbf{x}_{beam}(t) = \mathbf{W}\mathbf{x}(t), \quad (49)$$

$$[\mathbf{W}]_{s,t} = \frac{1}{\sqrt{\mathrm{K}}}e^{j\frac{2\pi}{P}(s-M-1)(t-1)}, \quad (50)$$

where $s = 1, \ldots, 2M+1$ and $t = 1, \ldots, P$. For estimating direction of arrival the Eigen decomposition and the beamspace data covariance matrix are calculated:

$$\mathbf{R} = E\{\mathbf{x}_{beam}(t)\mathbf{x}_{beam}^H(t)\} = E_S\Lambda_S E_S^H + E_N\Lambda_N E_N^H, \quad (51)$$

Where the diagonal matrices $\Lambda_S \in \mathbb{R}^{K\times K}$ and $\Lambda_N \in \mathbb{R}^{2M+1-K\times 2M+1-K}$ denote to the signal subspace and noise subspace eigenvalues of $\mathbf{R}$. The matrices columns $E_S \in \mathbb{C}^{2M+1\times K}$ and $E_N \in \mathbb{C}^{2M+1\times 2M+1-K}$correspond to eigenvectors of signal subspace and noise subspace respectively. The beamspace Multiple Signal Classification (MUSIC) algorithm [16] estimates the direction of arrival of signal from the K deepest nulls.

$$f_{music}(\theta_0,\varphi) = \mathbf{a}_{beam}^H(\theta_0,\varphi)E_N E_N^H\mathbf{a}_{beam}(\theta_0,\varphi), \quad (52)$$

Where $\mathbf{a}_{beam}(\theta_0,\varphi) = \mathbf{W}\mathbf{a}(\theta_0,\varphi)$. The azimuth angles are distinct now and can be separated. And the diversified array becomes

$$\mathbf{a}_{beam}(\theta_0,\varphi) = \mathbf{M}(z) = [\begin{matrix} a_{-M}^{\theta}(\theta_0)z^{-M} \ldots a_M^{\theta}(\theta_0)z^M \\ a_{-M}^{\varphi}(\theta_0)z^{-M} \ldots a_M^{\varphi}(\theta_0)z^M \end{matrix}]^T, \quad (53)$$

where $z = e^{j\varphi}$. The working of beamspace essentially takes advantage of the symmetrical nature of uniform circular array and spreads out the array diversity into distinct phase modes. The above equation (53) is only valid for P > 2M+1,

otherwise it will lead to mix up of phase modes.

From equations (52) and (53)

$$f_{music}(\theta_0, \varphi) = \mathbf{M}^H(z) E_N E_N^H \mathbf{M}(z) = \mathbf{C}(z), \quad (54)$$

To estimate the direction of arrival (DOA), it is observed that the smallest eigenvalue in equation (53) is always positive and nearby zero when interference is present where azimuthal angle φ approaches one of the perceived DOA's. Therefore DOA will be estimated by calculating estimates of z such that

$$\det\{\mathbf{C}(z)\} = 0, \quad (55)$$

The equation $\mathbf{C}(z)$ is a polynomial in z, therefore for finding the direction of arrival of plane wave, ROOT_MUSIC algorithm will be utilized since it can handle transformation in polynomial rooting. Hence all those roots of this polynomial that exist nearby the unit-circle redeem estimates in the required azimuth angles φ, i.e.,

$$\hat{\varphi} = \angle \frac{z}{|z|}, \quad (56)$$

Estimation of direction of arrival of the interferer using uniform circular array analytically promises excellent results.

III. CONCLUSION

In this paper, we have analyzed a deterministic model for cancelation of interference in an open space. The applicability of the adaptive algorithmic technique in a classic practical scenario is analyzed. Some of the main theoretical findings of this study are summarized below:

(1) By evaluating the power of various incoming signals, the transmitted signal will only be equal to the received signal without ambient noise in case if phase delay of $\frac{2\pi}{\lambda} D cos\theta$ is added to the signal that comes earlier at the antenna port. Therefore phase compensation is mandatory to measure EUT emissions only in the presence of interference signals.

(2) Diversity combining techniques as used in wireless communication for improving signal to noise ratio can be employed here e.g., maximal ratio combining (MRC) technique since it synchronizes the phases of multiple copies of signal received at different antennas without a priori information of the spatial installation.

(3) Estimation of direction of arrival of the interferer using uniform circular array analytically promises excellent results.

IV. ACKNOWLEDGMENT

The authors gracefully acknowledge advanced studies and research board (ASRB) UET Lahore for funding the project under No.DR/ASRB-83/211.

REFERENCES

[1] Svacina, J.; Drinovsky, J.; Videnka, R., "Virtual Anechoic Room An Useful Tool for EMI Pre-Compliance Testing," *Radioelektronika, 2007. 17th International Conference* , vol., no., pp.1-4, 24-25 April 2007.

[2] Jian Xu; Fei Dai; Donglin Su; Qi Qiao; Haopeng Zheng, "Ambient noise cancellation in frequency domain EMI measurement," *Microwave, Antenna, Propagation, and EMC Technologies for Wireless Communications (MAPE), 2011 IEEE 4th International Symposium on* , vol., no., pp.555-558, 1-3 Nov. 2011.

[3] Widrow, B.; Glover, J.R., Jr.; McCool, J.M.; Kaunitz, J.; Williams, C.S.; Hearn, R.H.; Zeidler, J.R.; Eugene Dong, Jr.; Goodlin, R.C., "Adaptive noise cancelling: Principles and applications," *Proceedings of the IEEE* , vol.63, no.12, pp.1692-1716, Dec. 1975.

[4] A. Frech, M. Klugel and P. Russer, "Adaptive filtering for noise cancellation and signal analysis in real-time," *Microwave Conference (EuMC), 2013 European*, Nuremberg, pp. 1123-1126, 2013.

[5] Mirchandani, G.; Zinser, R., Jr.; Evans, J.B., "A new adaptive noise cancellation scheme in the presence of crosstalk [speech signals]," *Circuits and Systems II: Analog and Digital Signal Processing, IEEE Transactions on* , vol.39, no.10, pp.681-694, Oct 1992.

[6] Awan, F.G.; Sheikh, N.M., "Model for Radiation Emission EMC Measurement at OATS: Issues and Approaches," *Measurement, Journal of the International Measurement Confederation* (IMEKO), vol. 42, issue 7, pp. 1045-1052, August 2009.

[7] Awan, F.G.; Sheikh, N.M.; Kiran, A., "Performance Evaluation of Open Space Interference Cancellation Model in EMC Measurement," *Science International Journal* **(**CODEN: SINTE 8**)**, vol. 26, issue 1, pp. 503-506, January 2014.

[8] Moreira, J.D.; Almenar, V.; Corral, J.L.; Flores, S.; Girona, A.; Corral, P., "Diversity techniques for OFDM based WLAN systems," *Personal, Indoor and Mobile Radio Communications, 2002. The 13th IEEE International Symposium on* , vol.3, no., pp.1008-1011 vol.3, 15-18 Sept. 2002.

[9] Razavi, S.M.; Ratnarajah, T.; Masouros, C.; Sellathurai, M., "Joint interference and phase alignment in multiuser MIMO interference channels," *Signals, Systems and Computers (ASILOMAR), 2012 Conference Record of the Forty Sixth Asilomar Conference on* , vol., no., pp.1137-1141, 4-7 Nov. 2012.

[10] Angerer, C.; Langwieser, Robert; Maier, G.; Rupp, M., "Maximal ratio combining receivers for dual antenna RFID readers," *Wireless Sensing, Local Positioning, and RFID, 2009. IMWS 2009. IEEE MTT-S International Microwave Workshop on* , vol., no., pp.1-4, 24-25 Sept. 2009.

[11] Shah, A.; Haimovich, A.M., "Performance analysis of maximal ratio combining and comparison with optimum combining for mobile radio communications with cochannel interference," *Vehicular Technology, IEEE Transactions on* , vol.49, no.4, pp.1454-1463, Jul 2000.

[12] Kyung Seung Ahn; Heath, R.W., "Performance analysis of maximum ratio combining with imperfect channel estimation in the presence of cochannel interferences," *Wireless Communications, IEEE Transactions on* , vol.8, no.3, pp.1080-1085, March 2009.

[13] Chen, Xiaoming. "Measurements and evaluations of multi-element antennas based on limited channel samples in a reverberation chamber." *Progress in Electromagnetics Research*, Pier 131, pp.45-62, 2012.

[14] Rogier H, Bonek E., "Analytical spherical-mode based compensation of mutual coupling in uniform circular arrays for direction-of-arrival estimation," *Int. Journal of Electr. and Comm.* vol.60, no.3, pp.179-189, March 2006.

[15] Mathews, Cherian P.; Zoltowski, M.D., "Eigenstructure techniques for 2-D angle estimation with uniform circular arrays," *Signal Processing, IEEE Transactions on* , vol.42, no.9, pp.2395-2407, Sep 1994.

[16] Schmidt, R.O., "Multiple emitter location and signal parameter estimation," *Antennas and Propagation, IEEE Transactions on* , vol.34, no.3, pp.276-280, Mar 1986.